Constraining primordial black hole masses with the isotropic gamma ray background

Alexandre Arbey, Jérémy Auffinger, Joseph Silk

Constraining primordial black hole masses with the isotropic gamma ray background

Alexandre Arbey[*]
Univ Lyon, Univ Claude Bernard Lyon 1, CNRS/IN2P3, IP2I Lyon, UMR 5822, F-69622 Villeurbanne, France

Jérémy Auffinger[†]
Institut d'Astrophysique de Paris, UMR 7095 CNRS, Sorbonne Universités, 98 bis, boulevard Arago, F-75014 Paris, France, Univ Lyon, Univ Claude Bernard Lyon 1, CNRS/IN2P3, IP2I Lyon, UMR 5822, F-69622, Villeurbanne, France, and Département de Physique, École Normale Supérieure de Lyon, F-69342 Lyon, France

Joseph Silk[‡]
Institut d'Astrophysique de Paris, UMR 7095 CNRS, Sorbonne Universités, 98 bis, boulevard Arago, F-75014 Paris, France, The Johns Hopkins University, Department of Physics and Astronomy, Baltimore, Maryland 21218, USA, and Beecroft Institute of Particle Astrophysics and Cosmology, University of Oxford, Oxford OX1 3RH, United Kingdom

(Received 10 June 2019; published 22 January 2020)

Primordial black holes (PBHs) can represent all or most of the dark matter in the window 10^{17}–10^{22} g. Here we present an extension of the constraints on PBHs of masses 10^{13}–10^{18} g arising from the isotropic diffuse gamma-ray background. Primordial black holes evaporate by emitting Hawking radiation that should not exceed the observed background. Generalizing from monochromatic distributions of Schwarzschild black holes to extended mass functions of Kerr rotating black holes, we show that the lower part of this mass window can be closed for near-extremal black holes.

DOI: 10.1103/PhysRevD.101.023010

I. INTRODUCTION

Primordial black holes (PBHs) are the only candidates able to solve the dark matter (DM) issue without invoking new physics. Two mass windows are still open for the PBHs to contribute to all or most of the DM: the 10^{17}–10^{19} g range, recently reopened by Ref. [1] after revisiting the γ-ray femtolensing constraint, and the 10^{20}–10^{22} g range [2], from hubble space telescope microlensing probes of M31. PBHs are believed to have formed during the post-inflationary era, and subsequently evolved through accretion, mergers and Hawking radiation (HR). If the PBHs were sufficiently numerous, that is to say if they contribute to a large fraction of DM, HR from PBHs may be the source of observable background radiation.

In this paper, we update the constraints on the number density of PBHs by observations of the diffuse isotropic gamma-ray background (IGRB) [3,4], taking into account the latest *Fermi-LAT* data [5] and, as new constraints, the spin of PBHs and extension of the PBH mass function (in the case of a log-normal distribution). Our assumption is that part of the IGRB comes from the time-stacked, redshifted HR produced by evaporating PBHs distributed isotropically in the extragalactic Universe. Those PBHs must have survived at least until the epoch of cosmic microwave background (CMB) transparency for the HR to be able to propagate in the intergalactic medium. This sets the lower boundary on the PBH mass $M_{\min} \approx 5 \times 10^{13}$ g. This statement is however mode dependent as quantum-gravity effects may accelerate the PBH evaporation and thus modify the time stacking of the corresponding emitted radiation [6]. Furthermore, the HR peaks at an energy which decreases when the PBH mass increases. This sets the upper boundary for the PBH mass $M_{\max} \approx 10^{18}$ g as the IGRB emission does not constrain the photon flux below 100 keV.

[*]alexandre.arbey@ens-lyon.fr
Also at Institut Universitaire de France, 103 boulevard Saint-Michel, 75005 Paris, France.
[†]j.auffinger@ipnl.in2p3.fr
[‡]joseph.silk@physics.ox.ac.uk

This paper is organized as follows. Section II gives a brief review of HR physics, Sec. III describes the IGRB flux computation and Sec. IV presents the new constraints obtained with Kerr and extended mass function PBHs.

II. KERR PBH HAWKING RADIATION

BHs emit radiation and particles similar to blackbody radiation [7] with a temperature linked to their mass M and spin parameter $a \equiv J/M \in [0, M]$ (J is the BH angular momentum) through

$$T \equiv \frac{1}{2\pi}\left(\frac{r_+ - M}{r_+^2 + a^2}\right), \tag{1}$$

where $r_+ \equiv M + \sqrt{M^2 - a^2}$ and we have chosen a natural system of units with $G = \hbar = k_B = c = 1$. The number of particles N_i emitted per unit energy and per unit time is given by

$$\frac{\mathrm{d}^2 N_i}{\mathrm{d}t\mathrm{d}E} = \frac{1}{2\pi}\sum_{\text{d.o.f.}} \frac{\Gamma_i(E, M, a^*)}{e^{E'/T} \pm 1}, \tag{2}$$

where $E' \equiv E - m\Omega$ is the total energy of the particle taking into account the BH horizon rotation velocity $\Omega \equiv a^*/(2r_+)$, $a^* \equiv a/M \in [0, 1]$ is the reduced spin parameter, m is the projection of the particle angular momentum l and the sum is over the degrees of freedom (d.o.f.) of the particle (angular momentum and color and helicity multiplicities). The $\pm$ signs are for fermions and bosons, respectively. The greybody factor $\Gamma_i(E, M, a^*)$ encodes the probability that a Hawking particle evades the gravitational well of the BH. It corresponds to the departure from pure blackbody radiation and is obtained as the ratio of the amplitude of a plane wave describing an elementary particle between the BH horizon and spatial infinity. The computation methodology of the greybody factors is well described in the literature and we use here the values given in the public code BlackHawk [8] used for this study.

This emission can be integrated over all energies to obtain equations for the evolution of both the PBH mass and spin [9]

$$\frac{\mathrm{d}M}{\mathrm{d}t} = -\frac{f(M, a^*)}{M^2}, \tag{3}$$

and

$$\frac{\mathrm{d}a^*}{\mathrm{d}t} = \frac{a^*(2f(M, a^*) - g(M, a^*))}{M^3}, \tag{4}$$

where

$$f(M, a^*) \equiv -M^2\frac{\mathrm{d}M}{\mathrm{d}t} = M^2\int_0^{+\infty}\sum_{\text{d.o.f.}}\frac{E}{2\pi}\frac{\Gamma(E, M, a^*)}{e^{E'/T} \pm 1}\mathrm{d}E, \tag{5}$$

$$g(M, a^*) \equiv -\frac{M}{a^*}\frac{\mathrm{d}J}{\mathrm{d}t} = \frac{M}{a^*}\int_0^{+\infty}\sum_{\text{d.o.f.}}\frac{m}{2\pi}\frac{\Gamma(E, M, a^*)}{e^{E'/T} \pm 1}\mathrm{d}E. \tag{6}$$

There are two main effects coming from the PBH spin that play a role in the IGRB constraints. First, a Kerr PBH with a near-extremal spin $a^* \lesssim 1$ radiates more photons than a Schwarzschild one ($a^* = 0$). This is due to the coupling between the PBH rotation and the particle angular momentum for high-spin particles, linked to the phenomenon of superradiance [9–11]. We thus expect the gamma-ray constraints to be more stringent due to the more important photon flux. Second, a near-extremal Kerr PBH will evaporate faster than a Schwarzschild PBH with the same initial mass due to this enhanced HR [12]. Moreover, the photon peak emission of Kerr PBHs is located at higher energies than the Schwarzschild one. These two effects mimic the radiation of a PBH with zero spin and smaller mass. Hence, we expect that the constraints for Kerr PBHs will be shifted toward higher PBH masses when the initial reduced spin parameter a_i^* increases.

III. ISOTROPIC GAMMA-RAY BACKGROUND

Many objects in the Universe produce gamma rays, such as active galactic nuclei and gamma-ray bursts [5]. The IGRB is the diffuse radiation that fills the intergalactic medium once all point sources have been identified and removed from the measured photon flux. This background might come from unresolved sources, or more speculatively from DM decays or annihilations. Figure 1 shows the IGRB measured by four experiments (HEAO-1+balloon, COMPTEL, EGRET and *Fermi*-LAT) over a wide range of energies between 100 keV and 820 GeV.

If we consider the simplifying hypothesis that DM is distributed isotropically at sufficiently large scales, then its annihilations/decays should produce, at each epoch of the Universe since transparency, an isotropic flux of photons. Thus, the flux measured along some line of sight should be the redshifted sum over all epoch emissions. In the case of PBH HR and following Carr *et al.* [3,4] we estimate the photon flux at energy E to be

$$I \equiv E\frac{\mathrm{d}F}{\mathrm{d}E} \approx \frac{1}{4\pi}n_{\text{BH}}(t_0)E\int_{t_{\min}}^{t_{\max}}(1 + z(t))\frac{\mathrm{d}^2 N}{\mathrm{d}t\mathrm{d}E}((1 + z(t))E)\mathrm{d}t, \tag{7}$$

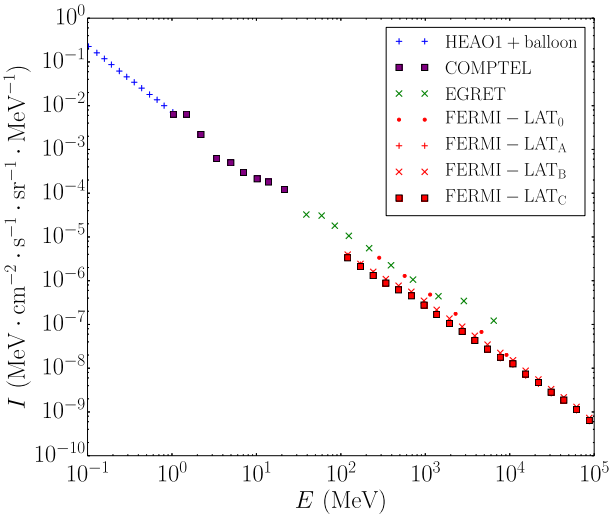

FIG. 1. The IGRB as measured by HEAO-1+balloon, COMPTEL, EGRET and *Fermi*-LAT missions [3–5]. The *Fermi*-LAT$_0$ marks correspond to the first-year results and the *Fermi*-LAT$_{A,B,C}$ marks correspond to six-year measurements.

where $n_{\rm PBH}(t_0)$ is the number density of PBHs of a given mass M today, $z(t)$ is the redshift and the time integral runs from $t_{\rm min} = 380\,000$ years at last scattering of the CMB to $t_{\rm max} = {\rm Max}(\tau(M), t_0)$ where $\tau(M) \sim M^3$ is the PBH lifetime and t_0 is the age of the Universe. As the Universe is expanding, the number density of PBHs evolves as $(1+z(t))^{-3}$, and the energy of the emitted photons evolves as $(1+z(t))^{-1}$. A last factor $(1+z(t))$ comes from the change of integrand variable from the line of sight to the present time. At $t > t_{\rm min}$, the Universe's expansion is dominated by the matter component and we have the relation

$$z(t) = (H_0 t)^{-2/3} - 1, \tag{8}$$

where H_0 is the Hubble parameter.

The HR emission spectrum $\mathrm{d}^2N/\mathrm{d}t\mathrm{d}E$ depends on the PBH mass and spin, and thus also on time as these quantities evolve through Eqs. (3) and (4). We also note the possibility that PBHs might be clustered at formation, leading to point-like gamma-ray sources and anisotropic spatial distribution. An unknown part of the resolved point-like sources of *Fermi*-LAT could be composed of small PBHs emitting HR [13], but these are removed from the IGRB, thus evading the constraints set here.

IV. RESULTS

We have used the new public code BlackHawk [8] to compute the HR of Eq. (2) and the PBH evolution given by Eqs. (3) and (4). We consider monochromatic PBH distributions of masses comprised between $M_{\rm min} = 10^{13}$ g and $M_{\rm max} = 10^{18}$ g and initial spin parameters between $a^*_{i,\rm min} = 0$ and $a^*_{i,\rm max} = 0.9999$, and compute the integral of Eq. (7) over the redshift (matter-dominated era)

$$z(t) = \left(\frac{1}{H_0 t}\right)^{2/3} - 1, \tag{9}$$

where H_0 is the present Hubble parameter. We then compare the result of the integral to the measured IGRB and find the maximum allowed value of the present PBH number density $n_{\rm PBH}(t_0)$ at a given PBH mass M, with a conservative approach taking into account the most stringent constraints (e.g., *Fermi*-LAT$_C$ at $E = 1$ GeV). The corresponding limit on the DM fraction f constituted of PBHs of mass M is obtained through $n_{\rm PBH}(t_0) = f\rho_{\rm DM}/M$, where $\rho_{\rm DM} \approx 0.264 \times \rho_{\rm tot} \approx 2.65 \times 10^{-30}$ g · cm^{-3} is the current average DM density in the Universe [14]. If the maximum allowed fraction f is greater than 1, we set it to 1 in order not to exceed the observed DM density, meaning that the IGRB does not constrain f for the given PBH mass.

High-spin PBHs may have been generated via scalar field fragmentation during a transient matter-domination period (e.g., Refs. [15,16]). Thus, observational limits linked to the spin of PBHs give a unique probe of these inflationary models. For the survival of such high spins, see e.g., Refs. [12,17].

A. Monochromatic PBH distribution

Figure 2 shows the resulting constraints for the DM fraction f in PBHs of mass M_* for initial spins $a^*_i \in \{0, 0.9, 0.9999\}$. First, we see that the $a^*_i = 0$ constraints are comparable with those of Ref. [3]. Our results do not exhibit the feature just after the peak linked to

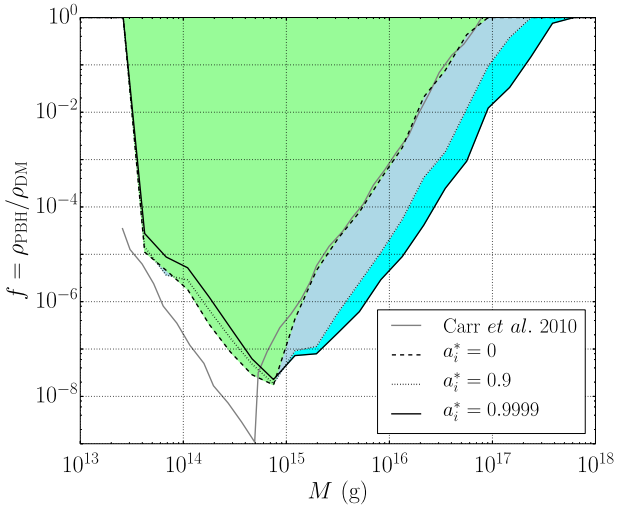

FIG. 2. The new IGRB constraints on the DM fraction f in the form of PBHs, for monochromatic distributions of PBHs of mass M_* and initial spins $a^*_i \in \{0, 0.9, 0.9999\}$. The shaded regions are excluded. For comparison, the result of Carr *et al.* [3] ($a^*_i = 0$) has been superimposed as a gray line.

primary-/secondary-photon domination explained in this article because we compute the secondary spectrum for all PBH masses. As a consequence, the peak is smoothed out. We see the second effect anticipated in Sec. II, that is to say the shifting of the constraint toward higher masses as the initial PBH spin parameter a_i^* increases. This is due to the fact that Kerr PBHs with high initial spin evaporate faster. Thus, in order to have the same kind of HR time distribution as a Schwarzschild PBH, the PBH must have a higher initial mass. However, this is not accompanied by a more stringent constraint linked to the enhanced emission for Kerr PBHs. We understand this as follows: PBHs with a higher mass emit photons at lower energies [cf. the temperature-mass relation (1)] where the IGRB constraints are less severe. The two effects approximately cancel. The main result that we find is that if PBHs have a high initial spin parameter $a^* \lesssim 1$, the "small-mass" window 10^{17}–10^{19} g can be reduced by up to almost 1 order of magnitude on its lower boundary, giving a narrower window of 6×10^{17}–10^{19} g for all DM into PBHs.

B. Extended PBH distribution

We also obtained constraints for extended mass functions to study the effects related to the width of a peak in the PBH mass distribution. Some pioneering work has been done in Refs. [18–21] concerning extended mass functions, predicting that the constraints on an extended distribution should be more stringent than the expected constraint resulting from the addition of monochromatic distributions. The conclusion of these papers is that a simple conversion from monochromatic to extended mass functions is not analytically trivial. We thus derive the extended mass function constraints by computing the full Hawking spectra associated to them before applying the constraints.

We considered extended mass functions of log-normal form

$$\frac{\mathrm{d}n}{\mathrm{d}M} = \frac{A}{\sqrt{2\pi}\sigma M}\exp\left(-\frac{(\ln(M/M_*))^2}{2\sigma^2}\right), \tag{10}$$

i.e., a Gaussian distribution in logarithmic scale for the density. A is some amplitude, linked to the fraction of DM into PBHs. This distribution is normalized for $A = 1$. To compute the spectra, `BlackHawk_tot` [8] was used with `spectrum_choice` $= 5$, and ten different PBH masses scanning the whole peak width.

We do not assume any model of PBH formation to justify this distribution, which is based on the fact that a Gaussian peak can mimic any peak in the PBH distribution resulting from a particular mechanism of formation, but we note that this mass distribution—with some variations—has been used in various works linked to different PBH formation mechanisms and mass ranges [13,22–28]. It may come from either a peak in the power spectrum of the primordial density inhomogeneities or a fragmentation during the collapse and initial clustering of the PBHs. We point out that extended distributions could have other shapes, e.g., a power law depending on their formation mechanism, but these are not studied here (see e.g., Ref. [27] for constraints on a power-law PBH distribution). To test these distributions, we have done a scan similar to the one described in the previous section, where M_* is the mean of the Gaussian distribution ranging from 10^{13} to 10^{18} g (cf. Sec. I for the PBH mass bounds), and its width $\sigma \in \{0.1, 0.5, 1\}$. Figure 3 shows examples of these distributions for $M_* = 3 \times 10^{15}$ g.

Equation (7) must be modified to obtain the fraction for an extended mass function. The flux is now given by

$$\begin{aligned} I &\approx \frac{1}{4\pi} E \int_{t_{\min}}^{t_{\max}} (1+z(t)) \frac{\mathrm{d}^2 n}{\mathrm{d}t\mathrm{d}E}((1+z(t))E)\mathrm{d}t \\ &\approx \frac{1}{4\pi} E \int_{t_{\min}}^{t_{\max}} (1+z(t)) \\ &\quad \times \int_{M_{\min}}^{M_{\max}} \left[\frac{\mathrm{d}n}{\mathrm{d}M}\frac{\mathrm{d}^2 N}{\mathrm{d}t\mathrm{d}E}(M,(1+z(t))E)\mathrm{d}M\right]\mathrm{d}t, \end{aligned} \tag{11}$$

with $\mathrm{d}n/\mathrm{d}M$ given by Eq. (10). The fraction of DM in the form of PBHs is obtained by maximizing this flux (increasing the normalization constant A) while respecting all the IGRB constraints, and is given by

$$f \equiv \frac{\rho_{\mathrm{PBH}}}{\rho_{\mathrm{DM}}} \tag{12}$$

$$= \frac{A}{\rho_{\mathrm{DM}}\sqrt{2\pi}\sigma}\int_{M_{\min}}^{M_{\max}} \exp\left(-\frac{\log(M/M_*)^2}{2\sigma^2}\right)\mathrm{d}M. \tag{13}$$

It is again limited to 1 in order not to exceed the DM content of the Universe. Even if the IGRB constraints valid

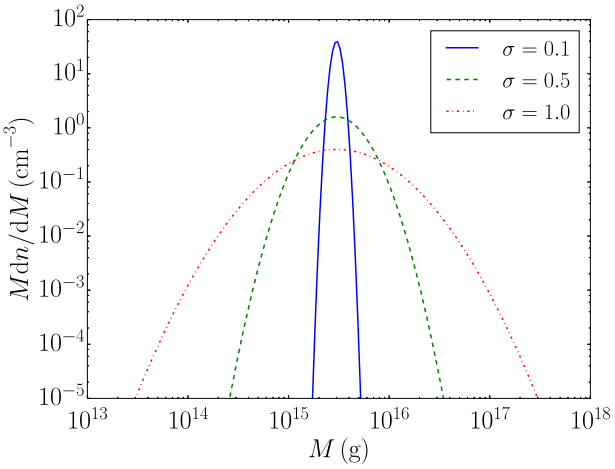

FIG. 3. Examples of distributions following Eq. (10) for values of $\sigma \in \{0.1, 0.5, 1\}$. The amplitude is $A = 1$ and the central mass is $M_* = 3 \times 10^{15}$ g for all distributions for clarity.

at M_* prevent A from exceeding its maximum value when $\sigma \to 0$ (monochromatic distribution), we expect that when the distribution width σ increases, monochromatic IGRB constraints from $M \lesssim M_*$ and $M \gtrsim M_*$ will become more and more important, thus limiting A. On the other hand, if σ increases, the full distribution integral that contributes to the DM fraction f increases as well because of the $M \lesssim M_*$ and $M \gtrsim M_*$ contributions. The competition between the two effects is difficult to forecast.

Figures 4(b), 4(c) and 4(d) show the constraints for distribution widths $\sigma \in \{0.1, 0.5, 1\}$ (respectively) and $a_i^* \in \{0, 0.9, 0.9999\}$. There are three kinds of observations to be considered.

(1) For a fixed PBH initial spin a^*, when the width of the distribution σ increases, the excluded region widens. This effect is sensible when $\sigma \gtrsim 0.5$. This can be interpreted as follows. When the PBH distribution is sharp, that is to say when their number density is concentrated in the central part $M \sim M_*$ of the distribution, then only the HR emitted by these central mass PBHs comes into play when applying the gamma-ray constraints, with the rest being negligible. Thus the constraints on f look very much like the monochromatic limit. When the distribution gets wider, the number density of PBHs is spread over $M > M_*$ and $M < M_*$ and these high- and low-mass PBHs (compared to the central value M_*) contribute more and more to the gamma-ray emission as σ, the width of the distribution, increases. As the constraints are most severe for $M_{\rm peak} \sim 10^{15}$ g, wide distributions centered on $M_* \ll M_{\rm peak}$ and $M_* \gg M_{\rm peak}$ for which the $M \sim M_{\rm peak}$ contribution is still important are severely constrained. At high σ, this extends the excluded region to $M_* \ll M_{\rm peak}$ and $M_* \gg M_{\rm peak}$ and closes the 10^{17}–10^{18} g window for all DM made of PBHs.

(2) For a fixed PBH initial spin a^*, when the width of the distribution σ increases, the constraint on f at the peak $M_{\rm peak}$ becomes less stringent. This is easily explained as follows. For a distribution peaked at $M_{\rm peak}$, the HR emitted by the PBHs of mass

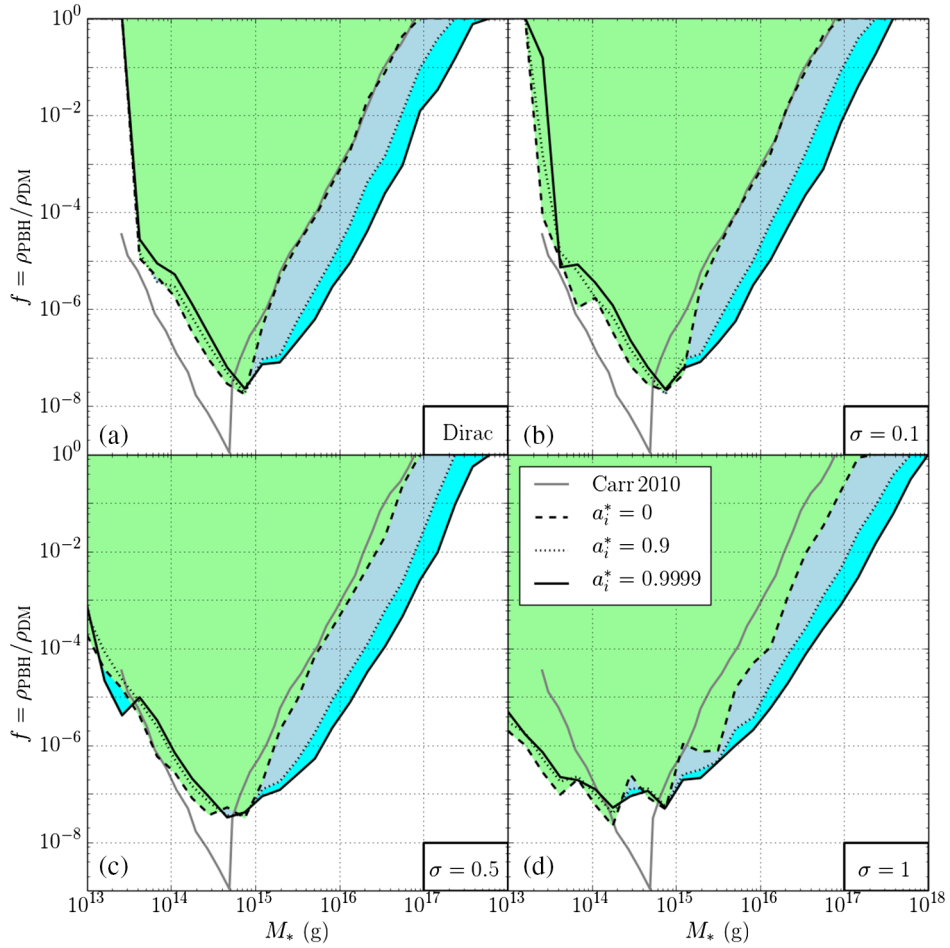

FIG. 4. Panel a: The same monochromatic plot as in Fig. 2 for comparison (here M_* is the monochromatic mass). Panels b, c, and d: The IGRB constraints on the DM fraction f in the form of PBHs, for distributions of PBHs of initial spins $a_i^* \in \{0, 0.9, 0.9999\}$ following Eq. (10), with central mass M_* and widths $\sigma \in \{0.1, 0.5, 1\}$ (b, c, d respectively). The shaded regions are excluded.

$M \sim M_{\rm peak}$ is the constraining part of the HR emitted by the full PBH mass distribution. Thus, adding PBHs with $M < M_{\rm peak}$ and $M > M_{\rm peak}$ to the distribution does not result in new HR constraints. However, the total number of PBHs increases, hence the maximum allowed fraction f of DM into PBHs increases.

(3) For a fixed width of the distribution σ, when the initial spin a^* of the PBHs increases, the constraints are shifted toward higher central masses while being slightly more stringent. This is coherent with the results of Fig. 4(a) for the monochromatic distributions presented in the previous section.

The oscillatory feature present on the constraint curves at $M \sim M_{\rm peak}$ is an artifact due to the discrete evaluation of the PBH mass distribution. Taking the convex hull of each shaded region should give a more robust conservative constraint.

We can sum up these observations in the following way. For an extended PBH mass function, the overall constraint comes from the PBHs evaporating today in this distribution with initial mass $M \sim M_{\rm peak}$. Distributions centered away from $M_{\rm peak}$ are more and more constrained as the tail of the distribution is important at $M_{\rm peak}$: f decreases as σ increases because the maximum value of A decreases. Distributions centered close to $M_{\rm peak}$ are not much more constrained when the distribution expands, as the maximum value of A remains the same: f increases as σ increases because the distribution integral increases. The very same effects can be observed in the right panel of Fig. 2 of Ref. [25].

With an extended mass function and no spin, the small mass window for all dark matter into PBHs reduces to 2×10^{17}–10^{19} g, and the addition of a nearly extremal spin parameter shrinks it to 10^{18}–10^{19} g, that is to say a loss of 1 order of magnitude compared to the previous zero-spin monochromatic distributions.

C. Comparison to other constraints

Recent studies have tried to close the very same mass range for PBHs constituting all of the dark matter, showing that this scenario is attracting much attention. Future femtolensing [1] or x-ray [29] surveys as well as current galactic positron data [25–27] and CMB anisotropies [28] all constrain the same $M = 10^{16}$–10^{18} g mass range.

Figure 5 compares the limits derived here and those based on galactic positrons [25,26] (we do not include the extended mass function limits of Ref. [27] because they result from a convolution of monochromatic limits with the mass function, a method which has limited applicability; see Sec. IV B). The limits obtained with a local measurement of the positron flux by *Voyager 1* [25], which has recently left the heliosphere and is capable of detecting low-energy positrons, are of the same order of magnitude as ours for widths $\sigma \lesssim 0.5$, while becoming significantly more stringent for $\sigma \gtrsim 1$. The limits derived from electron-positron annihilation in the

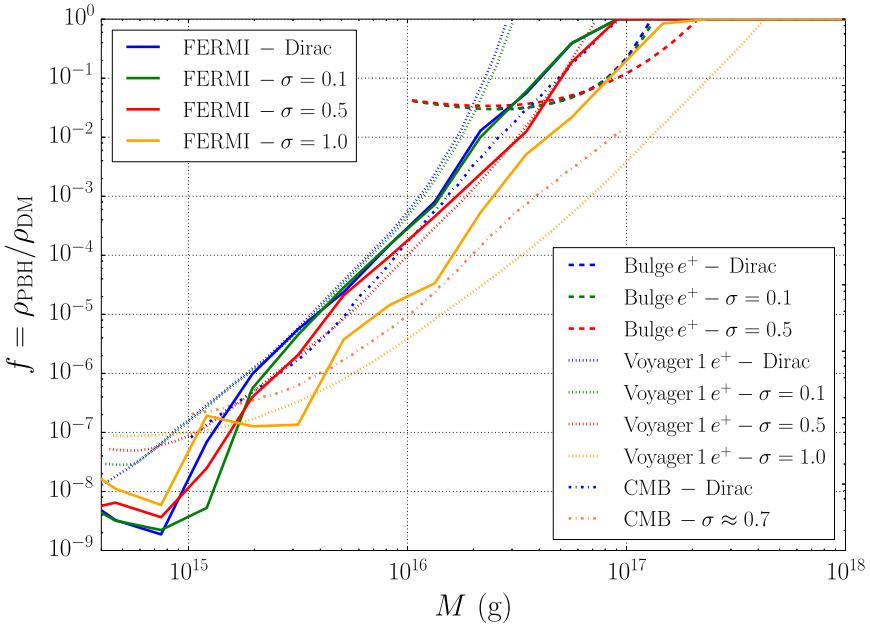

FIG. 5. Comparison between the limits derived in this work (solid lines) and those coming from electron-positron annihilations in the Milky Way bulge (dashed lines) [26], the local *Voyager 1* positron detections (dotted lines) [25] and the CMB anisotropies [28] (dash-dotted lines). Limits are shown for monochromatic mass functions (blue) as well as log-normal mass functions with Gaussian width $\sigma \in \{0.1, 0.5, 1\}$ (green, red and orange respectively). Reference [26] did not provide the $\sigma = 1$ data. Reference [28] used $\log_{10}$ normalizations, and thus their $\sigma_{10} = 0.3$ corresponds to a $\sigma \approx 0.7$ with our conventions, so it is marked with a slightly darker orange.

galactic bulge [26]—thus contributing to the 511 keV photon line—are more severe than the two others in the central mass region $M \sim 10^{17}$ g, but the authors claim that the *Voyager* limits are more restrictive when $\sigma \gtrsim 1$. The limits computed from CMB anisotropies [28], which are caused by the HR energy injection of light PBHs just before or during recombination, are of the same order of magnitude as the IGRB limits for the monochromatic distribution, but become more stringent for the $\sigma \approx 0.7$ data available. As those limits come from totally different galactic and extragalactic measurements, we consider them as interesting, independent and complementary, increasing the robustness of the conclusion concerning PBHs not constituting all of the DM in the 10^{16}–10^{17} g mass range.

V. CONCLUSION

In this paper, we have updated the IGRB constraint on PBH evaporation for monochromatic Schwarzschild PBH distributions, using the latest *Fermi*-LAT data and the new code BlackHawk. This has resulted in enhancing the constraint on the masses of presently evaporating PBHs, and reducing the constraint on $M_{\rm peak} \sim 10^{15}$ g. Our main result is the extension of the IGRB constraint from Schwarzschild to Kerr PBHs, and from monochromatic to extended mass functions. We have shown that increasing the initial spin parameter a_i^* of PBHs to near extremal values can close the mass window 10^{17}–10^{18} g (where PBHs could still represent all of the DM). We have also demonstrated that extended mass functions can allow a greater fraction of DM in the form of PBHs when they are centered close to the strongest monochromatic constraint $M_{\rm peak}$, while they are more severely constrained when centered away from this peak. In this case, the allowed mass window can be reduced even with Schwarzschild PBHs, complementing previous work in the same mass range with positron emission by evaporating PBHs.

ACKNOWLEDGMENTS

We would like to thank P. Graham and W. DeRocco for useful discussions.

[1] A. Katz, J. Kopp, S. Sibiryakov, and W. Xue, J. Cosmol. Astropart. Phys. 12 (2018) 005.
[2] H. Niikura, M. Takada, N. Yasuda, R. H. Lupton, T. Sumi, S. More, T. Kurita, S. Sugiyama, A. More, M. Oguri, and M. Chiba, Nat. Astron. **3**, 524 (2019).
[3] B. J. Carr, K. Kohri, Y. Sendouda, and J. Yokoyama, Phys. Rev. D **81**, 104019 (2010).
[4] B. Carr, F. Kühnel, and M. Sandstad, Phys. Rev. D **94**, 083504 (2016).
[5] FERMI-LAT Collaboration, Astrophys. J. **799**, 86 (2015).
[6] A. Raccanelli, F. Vidotto, and L. Verde, J. Cosmol. Astropart. Phys. 08 (2018) 003.
[7] S. W. Hawking, Commun. Math. Phys. **43**, 199 (1975).
[8] A. Arbey and J. Auffinger, Eur. Phys. J. C **79**, 693 (2019).
[9] D. N. Page, Phys. Rev. D **14**, 3260 (1976).
[10] S. Chandrasekhar and S. Detweiler, Proc. R. Soc. A **352**, 325 (1977).
[11] D.-C. Dai and D. Stojkovic, J. High Energy Phys. 08 (2010) 016.
[12] B. E. Taylor, C. M. Chambers, and W. A. Hiscock, Phys. Rev. D **58**, 044012 (1998).
[13] K. M. Belotsky, V. I. Dokuchaev, Y. N. Eroshenko, E. A. Esipova, M. Y. Khlopov, L. A. Khromykh, A. e. A. Kirillov, V. V. Nikulin, S. G. Rubin, and I. V. Svadkovsky, Eur. Phys. J. C **79**, 246 (2019).
[14] Planck Collaboration, arXiv:1807.06209.
[15] E. Cotner and A. Kusenko, Phys. Rev. D **96**, 103002 (2017).
[16] T. Harada, C.-M. Yoo, K. Kohri, and K.-I. Nakao, Phys. Rev. D **96**, 083517 (2017).
[17] A. Arbey, J. Auffinger, and J. Silk, arXiv:1906.04196.
[18] B. Carr, M. Raidal, T. Tenkanen, V. Vaskonen, and H. Veermäe, Phys. Rev. D **96**, 023514 (2017).
[19] F. Kühnel and K. Freese, Phys. Rev. D **95**, 083508 (2017).
[20] N. Bellomo, J. L. Bernal, A. Raccanelli, and L. Verde, J. Cosmol. Astropart. Phys. 01 (2018) 004.
[21] B. V. Lehmann, S. Profumo, and J. Yant, J. Cosmol. Astropart. Phys. 04 (2018) 007.
[22] A. M. Green, Phys. Rev. D **94**, 063530 (2016).
[23] K. Kannike, L. Marzola, M. Raidal, and H. Veermäe, J. Cosmol. Astropart. Phys. 09 (2017) 020.
[24] J. Calcino, J. García-Bellido, and T. M. Davis, Mon. Not. R. Astron. Soc. **479**, 2889 (2018).
[25] M. Boudaud and M. Cirelli, Phys. Rev. Lett. **122**, 041104 (2019).
[26] W. DeRocco and P. W. Graham, arXiv:1906.07740.
[27] R. Laha, arXiv:1906.09994.
[28] H. Poulter, Y. Ali-Haïmoud, J. Hamann, M. White, and A. G. Williams, arXiv:1907.06485.
[29] G. Ballesteros, J. Coronado-Blázquez, and D. Gaggero, arXiv:1906.10113.